ELSEVIER

Physica B 305 (2001) 233–241

PHYSICA B

www.elsevier.com/locate/physb

# Heat conductivity of $La_{1-x}Sr_xMnO_3$ surface layers

I. El-Kassab[a], A.M. Ahmed[a,1], P. Mandal[b], K. Bärner[a,*], A. Kattwinkel[a], U. Sondermann[c]

[a] *IV. Phys. Institut der Universität. Göttingen, Bunsenstr. 11-15, D-37073 Göttingen, Germany*
[b] *Saha Institute for Nuclear Physics, A-1F Bidhannagar, Calcutta 700064, India*
[c] *Institut für Mineralogie der Universität Marburg, Hans Meerweinstr., D-35039 Marburg, Germany*

Received 4 January 2001; received in revised form 28 May 2001

**Abstract**

Using the transient thermoelectric effect (TTE), we have measured the thermoelectric power $S(T)$ and the heat conductivity $\kappa(T)$ of $La_{1-x}Sr_xMnO_3$ ceramic surface layers with nominal compositions $x = 0.075$, 0.1, 0.15, 0.2 and 0.3 in the temperature range 50–340 K. Except for a shift in the characteristic temperatures, the surface layer $S(T)$ is still similar to the bulk thermopower while the heat conductivity $\kappa(T)$ is markedly different, even changing the slope at intermediate temperatures. As $S$ is less structure sensitive than $\kappa$, we relate these differences to an increased number density of defects near the surface. In particular, a stoichiometry gradient close to the surface and oxygen vacancy related (two level tunneling-) modes are indicated. In addition, new $S$ and $\kappa$ data are presented for lower doping, i.e. $x = 0.075$ and 0.1. 

*Keywords:* $La_{1-x}Sr_xMnO_3$; Surface layers; Thermal conductivity; Thermoelectric power

## 1. Introduction

The series $La_{1-x}Sr_xMnO_3$ is one of the most extensively studied system of giant magnetoresistance (GMR) compounds, mainly because of the high Curie temperatures which are obtained for higher Sr-contents [1–12,22–41]. However, if one hopes to use these ceramics as robust field sensors, the stability of the surface in air and eventual stabilisation measures become important. As with the TTE- or flash method, we measure the thermoelectric power $S$ and the heat conductivity $\kappa$ within the penetration depth of the applied light pulse, we can look at $\kappa$ and $S$ close to the surface. In particular $\kappa$ should show deviations from bulk data [1,17,36,37] and from the differences we may derive information about the (macroscopic) surface layer. We use the phase diagram [3] shown in Fig. 1 to sort out the bulk properties. With our choice of compounds, we intersect at $T_t$ ($x = 0.075$), $T_s$ ($x = 0.1$), $T_s \approx T_c$ ($x = 0.15$) and at $T_c$ ($x = 0.2$; 0.3), $T_t$ is a structural transition between two orthorhombic structures, $O \rightarrow O'$, $T_s$ supposedly a transition into a mixed state $O \rightarrow O/O'$ and $T_c$ a (double exchange) Curie temperature. We indeed find that the bulk/surface differences in $\kappa$ are larger as those in $S$, in particular in the vicinity of the various transitions.

*Corresponding author. Fax: +49-551-394560.
*E-mail address:* baerner@ph4.physik.uni-goettingen.de (K. Bärner).
[1] Physics Department, South Valley University, Sohag, Egypt.

0921-4526/01/$ -see front matter 
PII: S0921-4526(01)00618-4

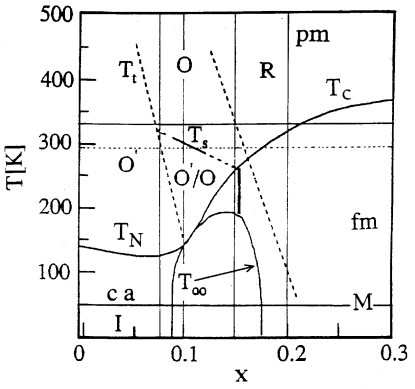


Fig. 1. Magnetic phase diagram of $La_{1-x}Sr_xMnO_3$: $T_c$, Curie temperature, ferromagnet; $T_N$ canted antiferromagnet, $T_t$ structural orthorhombic O/orthorhombic O′ transition; $T_s$ transition into a phase mixture $O \rightarrow O/O'$, $T_{oo}$ orbital and charge ordering transition.

## 2. Experimental and preparation

### 2.1. Preparation

The samples were made by standard ceramic techniques: in particular, high purity powders of $La_2O_3$, $SrCO_3$, and $MnO_2$ were mixed thoroughly and then fired at temperatures between 1400°C and 1500°C in air for several days with intermediate grindings. Finally, the powders were pressed into pellets and heated at 1500°C for two days. As compounds with low $x$ have a tendency to adopt an oxygen content more than three if prepared in air, the $x = 0.075$ sample was prepared in an argon atmosphere, but using the same heat treatment.

### 2.2. Characterization

The samples were then subjected to powder X-ray diffraction at room temperature. The lattice parameters are collected in Table 1 and coincide reasonably well with the literature. In particular, from the diffraction spectra we could detect the first structural transition line ($T_t$) $O' \rightarrow O$, ($x = 0.075$ and 0.1) while our data did equally well fit to an orthorhombic or rhombohedral cell for $x > 0.1$, making it impossible to confirm the second structural transition line $O \rightarrow R$. However, in Table 1 we have choosen the lattice parameters such as to comply with the symmetries as proposed in Fig. 1. Bulk resistivity measurements were performed in a cryostat using the standard four-point method. Fig. 2 shows the resistivity versus temperature curves $\rho(T)$ for four of the compounds, i.e. $x = 0.075$, 0.1, 0.15, 0.2. Values of $\rho$ at 300 K are collected in Table 2. Note the change from purely activated behaviour ($x = 0.075$) to the typical metallic behaviour below the metal–insu-

Table 1
The lattice parameters[a]

| $x$ | $a$ (300 K) (nm) | $b$ (300 K) (nm) | $c$ (300 K) (nm) | Symmetry |
|---|---|---|---|---|
| 0.075 | 0.55464(9) | 0.56373(5) | 0.77251(9) | |
| | 0.5535 | 0.5650 | 0.7741 | O′ |
| 0.1 | 0.55333(8) | 0.55956(3) | 0.77101(4) | |
| | 0.5526 | 0.5613 | 0.7760 | O |
| 0.15 | 0.55290(5) | 0.55912(5) | 0.77108(8) | |
| | 0.5517 | 0.5550 | 0.7788 | O |
| 0.2 | 0.55305(5) | 0.55305(5) | 1.33689(4) | R |
| | 0.5496 | 60.62° | | |
| 0.3 | 0.55073(7) | 0.55073(7) | 1.33622(1) | R |
| | 0.5483 | 60.35° | | |

[a] Lower set of lattice parameters : Ref. [32].

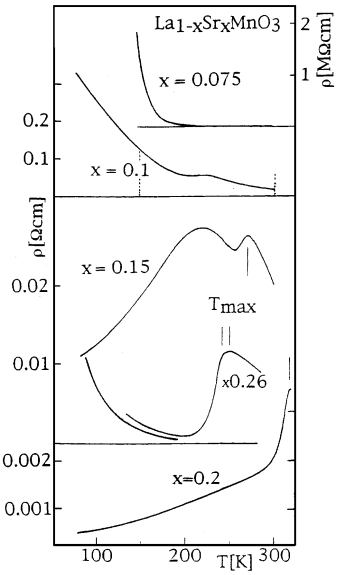


Fig. 2. Resistivity versus temperature curves $\rho(T)$ of $La_{1-x}Sr_xMnO_3$ compounds with $x = 0.075$, 0.1, 0.15, 0.2, 0.3, $T_{max} = T_c$ characteristic temperature; for more details see text.

Table 2
Values of $\rho$, $\kappa$ and $L$ at 300 K

| $x$ | $\rho$ (300 K) ($\Omega$ cm) | $\kappa$ (300 K) (W/km) | $L$ (300 K) (W $\Omega$/K$^2$) |
|---|---|---|---|
| 0.075 | 324 | 2.04 | $2.2\times10^{-2}$ |
| 0.1 | 0.015 | 1.40 | $0.7\times10^{-6}$ |
| 0.15 | 0.020 | 1.55 | $1.03\times10^{-6}$ |
| 0.15 | 0.030[a] | 1.15[a] | $1.15\times10^{-6}$ |
| 0.2 | 0.0021 | 1.61 | $1.13\times10^{-7}$ |
| 0.3 | 0.0014[b] | 2.47 | $1.16\times10^{-7}$ |

[a] Ref. [1].
[b] Ref. [32].

lator transition and onset of ferromagnetic order ($T_{mi} = T_c$) for $x = 0.2$, in accord with the literature. The compound with nominal $x = 0.1$, although showing some anomalous behaviour could well be insulating for all temperatures as the structure around 225 K could be a secondary resistivity peak like the anomaly observed with $x = 0.15$ below $T_c$. This extra structure, which only occurs in polycrystals, probably has to do with grain boundaries [14]. For nominal $x = 0.15$, we compare our data with that of a single crystal [1]. Note, that our $T_c$ is a little higher, probably due to small deviations from the nominal composition in either case, but the secondary maximum is indeed absent in the single crystal. $\rho(T)$ of $x = 0.2$ does not show that extra hump distinctly. Note, that this extra (grain boundary) scattering anomaly makes a discrimination between metallic and semiconducting state through the slope of $\rho(T)$ impossible, at least in the case of ceramics. However, even with the single crystal one cannot easily detect an (eventual) metallic range. Thus, an independent indicator of the metallic state, for example the thermopower or the absence of space charges would be highly desirable. That the latter is possible using TTE-transients has been demonstrated with epitaxial layers [15] and would be, if properly developed, an important tool for determining the conduction state—metallic or insulating—also in ceramics.

### 2.3. TTE-method

In a TTE set-up a light pulse which is limited in space and time is applied close to one of the long ends of a thin rectangular sample (flash method). Contacts (usually silver paint) are applied to both sample ends and a (decaying) voltage is measured between them. Details of the experimental set-up used have been described in detail elsewhere [4], in particular tests using standard materials and perpendicular heat flow corrections have been performed [42,43]. In the current experiments the data aquisition is performed using Labview 5.2. In the case of a thermal diffusion, the initial amplitude $V_3$ of a TTE-transient is recorded, which is proportional to the thermopower $S$, while the decay time is related to the heat diffusivity $D$. The absolute thermopower cannot be obtained, as after applying the contacts one has build a thermochain, usually Cu–silver glue–sample-silver glue–Cu. Empirically, i.e. by comparing $V_3$ with conventionally measured thermovoltages, this gives a small positive linear contribution $S_c$ which has to be subtracted, i.e. $S_{exp} = S + S_c$. In addition, we do not measure with a constant temperature increment $\Delta T$ but with constant applied heat $\Delta Q$. Thus, before one can subtract this contribution one has to correct $V_3$ for the temperature increment. Using a constant light pulse, it is suggested to use $\Delta Q = c_p \Delta T$ for the correction, i.e. as we measure $V_3(T) = S\Delta T$, only the product $V_3 c_p/c_p(300\,\mathrm{K}) = V_3^*$ is proportional to $S_{exp}$. If $V_3$ is not too small, our corrected signal $V_3^*$ follows the conventionally measured TEP already, so that arguments concerning structure in $S(T)$ can be made without the contact correction. However, the best procedure is to calibrate the corrected TTE-data using conventional data from other sources. All this has been done. As an example we present $S(T)$ of a $La_{0.7}Ca_{0.3}MnO_3$ ceramic (Fig. 3). Note the small peak at the Curie temperature $T_c$, which remains if we use a Debye-function for $c_p(T)$ only. If we use experimental $c_p(T)$ data, this peak vanishes as it coincides with the specific heat peak (weak solid line). There remains a small dip which could be due to overestimating the $c_p$-peak. If one wants to resolve critical fluctuations in $S(T)$ one would have to choose the same sample quality and the same heat influx as with the $c_p(T)$ measurement. The specific heat capacity $c_p \approx c_v$, which we use for the $V_3 \to S$ conversion, is also needed to calculate the heat conductivity from the heat

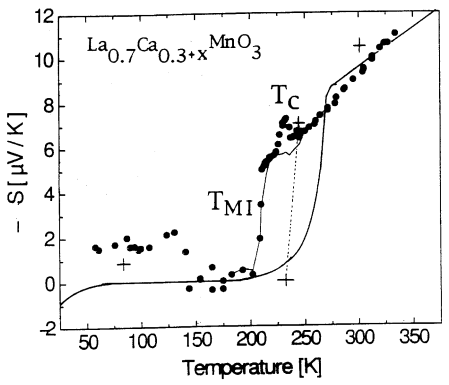


Fig. 3. Thermopower $S(T)$ of $La_{0.7}Ca_{0.3+x}MnO_3$: ●, $x = 0$; $c_p(T)$: Debye-function, TTE-method; —, $x = 0$, experimental $c_p(T)$, TTE-method; +, $x = 0$, conventional TEP; —, $x = 0.03$ acc. to Ref. [35]; $T_c$, $T_{mi}$: Curie temperature, metal–insulator transition temperature.

diffusivity $D$, since $D = \kappa/\rho_0 c_v$ ($\rho_0$: density). $\kappa$ is the simpler quantity from a theoretical point of view and in general compares easier with the literature. The $c_p(T)$ data on these particular samples were obtained using a standard DSC-2 Perkin–Elmer calorimeter and are not supposed to be surface sensitive aside from a possible shift of $T_c$ due to the slight oxygen non-stoichiometry.

Thus, while we can have a marker for the magnetic transition using a constant heat pulse $\Delta Q$, we cannot hope to unambiguously separate critical fluctuations. Note also the sharp drop in $S(T)$ at a temperature below $T_c$, suggesting that here the magnetic transition (at $T_c$) and the metal–insulator transition are slightly different, $T_{mi} < T_c$. The strong solid line represents a conventional measurement of $S(T)$ of $x = 0.33$, taken from the literature [38], while the crosses denote our own calibrating conventional bulk TEP-measurement on a sample from the same batch. While the shape and magnitude of $S(T)$ is similar in general, the MI-transition appears to be shifted and might even coincide with $T_c$ for bulk $x = 0.3$ and 0.33. This suggests different oxygen deficits $\delta$ in the bulk and in the surface layer. $\delta$ might increase the carrier density through changing the disproportion, but it also blocks certain Zener bonds via its oxygen defect sites [41], thus, reducing the Curie temperature and eventually even splitting $T_c$ and $T_{mi}$. From the $T_{mi}$ shift one can estimate the largest oxygen deficiency to be about 1%. The curves also suggest that the shift of transition temperatures with increasing A-doping $x$ is opposite to that of increasing oxygen deficiency.

As the TTE-method works best with thin layer samples and as near the surfaces the oxygen content might differ from that in the bulk, with thicker samples the TTE-method has to be considered *surface sensitive* as compared to conventional (bulk) methods. The penetration depth of the light and with it the pertinent layer depth measured, is here likely given by the halogen lamp quartz glass IR-cutoff, i.e. $\leqslant 4\,\mu m$. Moreover, because of the small temperature gradients we use, generally both $S(T)$ and $\kappa(T)$ show sharper structure as compared to conventional measurements, in particular if there one uses larger sample volumes, which usually adds compositional inhomogeneity.

Since we usually apply an impedance transformer, $S$ can be measured also with higher impedance samples where conventional TEP-setups suffer from stray induction voltages.

In the case of semiconductors, one can have two additional and faster transients, i.e. internal electric fields resulting from ambipolar diffusion of electron–hole pairs which are excited over an energy gap, $V_1(t)$, and, following this excitation, the decay of internal space charges captured in trap states $V_2(t)$ [13]. Therefore, for the semiconducting regions of the La–Sr samples we have occasionally scrutinized the initial part of the transients. For $x = 0.1$ in particular, we have tried to find a second transient. For that, the signal to noise ratio was enhanced through transient repetitions and averaging: only at low temperatures, $T < 80\,K$, we find indications for an additional faster transient but its amplitude is less than 5% of $V_3$. Thus, to date we can only state that the compound with $x = 0.1$ is insulating at 59 K, consistent with the phase diagram and the observed resistivity and thermopower (see Figs. 2 and 4).

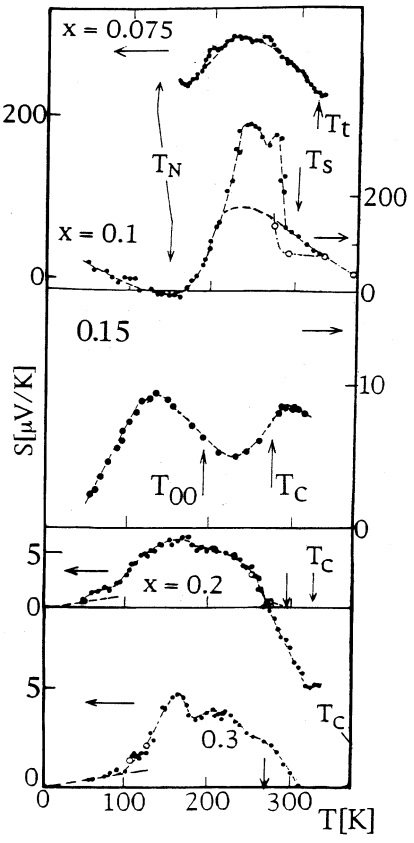


Fig. 4. Thermopower $S(T)$ for $x = 0.075$, 0.1, 0.15, 0.2, 0.3 solid points: this work; open points: [25], undesignated arrows: zero crossings acc. to Ref. [25].

## 3. Results and discussion

### 3.1. Thermoelectric power

Bearing in mind that we can have a fm- metal to pm- insulator transition, for the ferromagnetic metallic range we expect diffusion thermopower $S_d \sim T$ [18], superimposed to a magnon thermopower contribution $S_m$ [33], while for the activated regime one has a choice between the standard semiconductor expression $S = (k/e)(\Delta E/kT + c_2)$; $\Delta E$: energy gap, $c_2 \approx$ constant [19] and the polaron thermopower [3,20,21,35,44]. In addition, one has to consider the eventuality of a two carrier situation and one also has to remember that always $S \to 0$ for $T \to 0$, according to the third law of thermodynamics.

The overview of $S(T)$ for the various compounds (Fig. 4) suggests as trends:

(1) an increase of $S$ on going from the metallic to the semiconducting regimes, as expected.
(2) a negative or zero slope of $S(T)$ in the semiconducting regimes, like predicted above, while for the metallic regimes $S_m$ appears to be the dominant contribution.

On that basis, we have tentatively evaluated $\Delta E/k$ and $E_F/\xi$ ($\xi$: logarithmic energy dependence of the resistivity [18]; $E_F$ Fermi energy), after calibrating $S(T)$ with literature data [3,12,25,33]. The gap values $\Delta E$ would be between 10 and 20 meV, which is even lower as those formally derived from $\rho(T)$, i.e. 20–25 meV [22], suggesting the use of a two carrier and/or a hopping model. The weighted Fermi energies $E_F/\xi$ lie around 8–9 eV. According to band calculations $E_F$ lies indeed between 6.8 and 7.8 eV [23,24].

#### 3.1.1. Thermopower of $La_{0.85}Sr_{0.15}MnO_3$

For a more detailed discussion we start with $x = 0.15$. We find in particular a slight decrease for $T > T_c$, i.e. in the paramagnetic and insulating region. However, at $T < T_c$ a drop occurs, suggesting a metal to insulator transition. At the orbital ordering, $T_{oo}$, $S(T)$ rises again like in Refs. [1,3,33], suggesting that insulating behaviour reappears. The arrows denote the bulk transition temperatures taken from Fig. 1. Note, that our characteristic temperatures ($T_{oo}$, $T_c$) appear shifted, consistent with the idea of surface layer modified properties.

#### 3.1.2. Thermopower of $La_{0.9}Sr_{0.1}MnO_3$

For this compound, around 250 K a very prominent double peak occurs. As indicated by the open points, the ascending slope is also reported for bulk ceramic [25], and again our characteristic temperatures appear to be shifted against the bulk values. While the peak at higher temperatures might relate to critical fluctuations, as the O′ phase appears at $T_s$, the origin of the second peak is unknown. It might have to do with the changing volume fractions of O′/O, eventually

in interaction with the grain boundaries. In the middle of that region, i.e. at 225 K, the volume fractions would be equal, and eventually equal to the grain size, thus making up thermochains of pockets of O and O′ phases, which might result in a higher TEP as compared to that of the individual homogeneous phases when distributed inside the grains. At $T_s$ and $T_N$ (transition into a canted magnetic order) the phase mixture apparently reduces to a single phase. Support for a phase separation itself comes from the fact that while at temperatures above the double peak $S(T)$ is stable in respect to different temperature runs, we observe a degradation of $S(T)$ in the temperature range $T_N < T < T_s$. The structures do not disappear but they tend to broaden out, indicating temperature cycle induced structural changes—the data given in Figs. 4 and 5 are averages over 3 temperature runs. This partly irreversible behaviour is not found in the neighbouring compounds $x = 0.15$ and 0.075, again supporting the suspected O/O′ phase mixture. For $T < T_N \approx 150$ K, the situation is again stable. For that region, from $S(T)$ we can deduce insulating behaviour, but we cannot extract a gap value because of the zero crossing(s) around 150 K.

### 3.1.3. Thermopower of $La_{0.925}Sr_{0.075}MnO_3$

If we move to $x = 0.075$, the sample should be insulating everywhere; however, we would expect an influence of the structural transition $T_t$; apparently this is small, as we observe neither critical fluctuations nor a change of slope close to $T_t$. While the slope of $S(T)$ is negative at high temperatures as with $x = 0.1$, at intermediate temperatures it is positive. As $S$ is sensitive to changes in electronic state, while the compound certainly remains insulating in this temperature interval, we may connect this anomaly with a continuous change in the electronic structure, eventually an increasing carrier localisation when we approach $T_N$, which would be consistent with the steeply rising $\rho(T)$. Similar changes seem to occur also with $x = 0.1$ (dashed line), contributing to the steep drop of $S(T)$ to small negative values. All this would suggest that $T_N$ is not a simple Neel temperature, but more similar to a charge and orbital ordering temperature, which in turn would

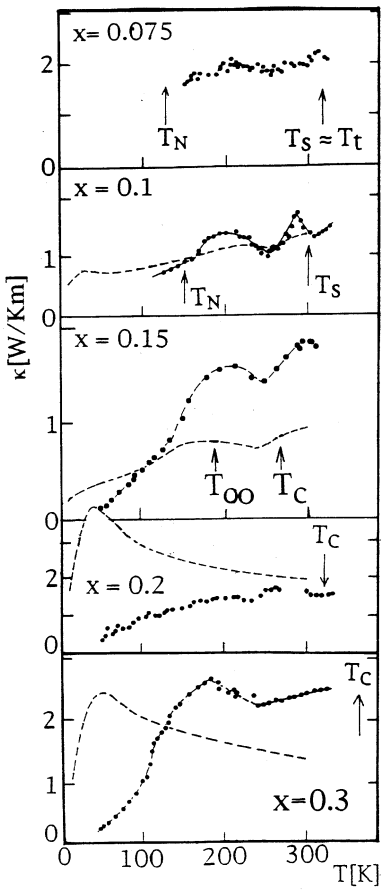


Fig. 5. Heat conductivity $\kappa(T)$ for $x = 0.075, 0.1, 0.15, 0.2, 0.3$: dashed lines acc. to Ref. [37], multiply by $f(x)$ to fit $\kappa$-scale: $f(x = 0.11) = 1.58$; $f(x = 0.155) = 2.5$; $f(x = 0.2) = 1.95$; $f \times (x = 0.3) = 3.4$.

suggest a crossing over of the $T_c$ and $T_{oo}$ phase lines, similar to the theoretical phase diagram as put forward in Ref. [2].

### 3.1.4. Thermopower of $La_{0.8}Sr_{0.2}MnO_3$ and $La_{0.7}Sr_{0.3}MnO_3$

With $x = 0.2$, we enter the regime of metallic conduction and thus should generally measure lower thermovoltages. This is indeed found. When we compare our samples with those of nominally the same composition [25], we again observe relative shifts in the zero crossing temperatures (arrows in Fig. 4) up to 40 K, again suggesting surface layer and/or compositional difference related shifts. We find hump-shapes of $S(T)$ in

the metallic regime of both compounds which are probably magnon contributions [27,28,33]. Then small structures on this humps are real, they could relate to specific magnon branches or, considering the strong magnon–phonon coupling in these compounds, to specific phonon branches. Interestingly, they appear to be more pronounced in our data as compared to bulk data [25,33], suggesting a surface layer changed phonon spectrum. Similar low temperature structures were observed for $x = 0.18$ [34]. At low temperatures the thermopower seems to become linear, suggesting a numerical take over of the diffusion thermopower. If we tentatively attribute the linear contribution to a linear diffusion thermopower $S_d$ alone, for the metallic compounds we can obtain an estimate for the weighted Fermi energies (see Table 2). The zero crossing temperatures, which apparently always precede $T_c$, on the other hand point to a two carrier model.

### 3.2. Heat conductivity

In the case of magnetic materials, the heat conductivity can be written as a sum of heat conductivities arising from the lattice, the electronic system and the spin system [16]: $\kappa = \kappa_l + \kappa_e + \kappa_m$. The temperature dependence of the lattice contribution $\kappa_l$ usually goes over a broad maximum, since $\kappa_l \to 0$ for $T \to 0$ and $\kappa_l \sim T^{-n}$ at high temperatures where phonon-phonon (umklapp-) processes dominate the lattice heat conduction. In the case of amorphous materials or polycrystals, the broad maximum can degenerate to a shallow maximum or $\kappa(T)$ might be simply saturating at high temperatures, i.e $d\kappa/dT \geqslant 0$ for all $T$ [29]. Evidence for a significant electronic contribution can be derived from the effective Lorenz number $L = \kappa_e/\sigma T$ and in the case of metal insulator–transitions (at $T_{MI}$), eventually from a step at $T_{MI}$. The overview of $\kappa(T)$ for the various compounds (Fig. 5) suggests as trends:

(1) at temperatures between 50 and 150 K, the slope of $\kappa(T)$ is positive, suggesting a chemically or elastically randomized system, probably a distorted or oxygen deficient surface layer.
(2) the absolute values of $\kappa$ increase by a factor of 3 on going from $x = 0.1$ to 0.3 (factor of 8 acc. to Ref. [37]).
(3) a hump-like structure of variable height is observed between 100 and 250 K for all $x$.
(4) the phase transition temperatures do not show very distincly except for the onset of the (O/O′)-phase mixture ($T_s$).

As the increase in $\kappa$ with $x$ might have to do with the increased doping, we have calculated the effective Lorenz numbers $L = \kappa\rho/T$ at 300 K (Table 2) and find them to approach $L_o = 2.45 \times 10^{-8}\,\mathrm{W\,\Omega/K^2}$ with increasing $x$, as expected; however, even with the best conducting (semi-) metallic compound, $x = 0.3$, $L$ is only $1.15 \times 10^{-7}\,\mathrm{W\,\Omega/K^2}$, suggesting that $\kappa_e$ plays a minor role even in the fm metallic state of the manganites and cannot be held responsible for the general increase in $\kappa$ with $x$. In particular, the small step of $\kappa$ at $T_c$ of $x = 0.2$ suggest an electronic contribution of maximal $\kappa_e \leqslant 0.4\,\mathrm{W/Km}$ near $T_c$ for $x = 0.2$. For $x = 0.15$, $\kappa_e$ has been estimated to be 0.15 W/Km [1]. The magnon part is usually considered to be the smallest and its existence can be most easily concluded if there is structure at the magnetic transition $T_c$ or a magnetotransport effect. For $x = 0.17$ a magnetotransport change of 25% is observed applying a 9 T field [36] and one of 50% under 4 T for $x = 0.15$ [1]. However, these changes are not confined to $T_c$ and thus cannot be readily assigned to $\kappa_m$. One has to suspect field-induced changes in the bandstructure [30] or in the phonon spectra via magnetostrictive effects.

#### 3.2.1. Heat conduction of $La_{0.8}Sr_{0.2}MnO_3$ and $La_{0.7}Sr_{0.3}MnO_3$

For the bulk versus surface discussion of the individual $\kappa(T)$ we start with $x = 0.3$ and 0.2. As there is no significant step at $T_{mi} = T_c$ ($x = 0.2$), both $\kappa_e$ and $\kappa_m$ are small or they compensate. As $\kappa_m$ is supposed to be small, they are both small and then the lattice contribution should be dominant, resulting in the classical broad hump shape for the bulk heat conductivity—see dashed line in Fig. 5. Our almost continuous increase of $\kappa(T)$ deviates markedly, suggesting a surface layer related

property change. The structure in $\kappa(T)$ observed for $x = 0.3$, in particular suggest a specifically modified phonon spectrum. As we suspect an oxygen deficiency in the surface layers of our samples, in particular a connection with oxygen defect oscillations is indicated.

*3.2.2. Heat conduction of $La_{0.85}Sr_{0.15}MnO_3$*

The general shape of $\kappa(T)$ again suggests a dominant lattice contribution. However, now we have structure which is located definitely below $T_c$. As there is an equivalent peak for $x = 0.3$ and 0.1, we tend to connect this anomaly with oxygen deficiency modes, as above. Single crystals with $x = 0.15$ and 0.17 also show structure in $\kappa(T)$ in this temperature interval [1,36]. As the shape of the anomalies is somewhat different for ceramic and single crystal, grain boundaries could play a role, too. Fujishiro et al. have connected the general increase of $\kappa$ with $x$ with the $O \rightarrow R$ symmetry change, when certain oxygen related anomalous two-level phonon modes become less important (in the R-structure), and thus the heat conduction in that structure is increased.

Interestingly, their $x = 0.15$ sample also shows (a double hump) structure [37], suggesting a relation between these humps and the compositionally based reduction in $\kappa$. Obviously, these structures become more pronounced in the surface layers. However, because of the random arrangement of the defects it is unlikely that the surface layer undergoes a symmetry change. As the structures in $\kappa(T)$ also appear in different magnitude for different samples and compositions, we tend to assign them to (oxygen) defect modes. Still, the general trend $\kappa(x)$ might be an intrinsic property (intrinsic oxygen modes).

*3.2.3. Heat conduction in $La_{0.9}Sr_{0.1}MnO_3$*

The O/O′ phase mixture, which, according to the phase diagram (Fig. 1) starts at $T_s$ should show for $x = 0.1$ only. Consequently, we connect the high temperature anomaly near $T_s$ with this phase mixture. In a (magnetically) inhomogeneous amorphous system a similar anomaly has been observed in $\kappa(T)$ and was connected with thermally excited magnetic clusters just below $T_c$, interfering with the heat conduction in the matrix, which in the absence of these excited clusters, i.e. both in the magnetically ordered and in the paramagnetic state, was assumed to be practically constant [31]. The phase mixture below $T_s$ of $x = 0.1$ would then be an example of an equivalent (structurally) inhomogeneous system.

*3.2.4. Heat conduction in $La_{0.925}Sr_{0.075}MnO_3$*

For the compound with $x = 0.075$, there is no phase mixture and we do not expect a peak-like anomaly near $T_s \approx T_t$, like that of $x = 0.1$. This is indeed observed. Also, consistent with the small structure if any of $\kappa$ at the structural transition $T_t$, we do not find a significant dependence on eventual lattice parameter changes below $T_t$ [26].

## 4. Summary

Using the flash method to measure the heat conductivity $\kappa$ and the thermoelectric power $S$ of $La_{1-x}Sr_xMnO_3$ ceramic, we detect a macroscopic surface layer where some physical properties are significantly changed. While $S(T)$ still follows the bulk data save for a shift of the characteristic transition temperatures, $\kappa(T)$ is notably different, suggesting a markedly changed phonon spectrum close to the surface. The strong sensitivity of the absolute values of $\kappa$ to oxygen-related modes in particular suggests that both the shift and the spectral changes are primarily connected to a gradient of the oxygen content close to the surface.

## Acknowledgements

The authors thank the Deutsche Forschungsgemeinschaft and the Alexander von Humboldt foundation for their support and E. Schmitt and E. Gmelin for some of the measurements. We also acknowledge the support of the Nato-linkage Grant PST.CLG 975703.

## References

[1] S. Uhlenbruck, B. Büchner, R. Gross, A. Freimuth, A. Maria de Leon Guevara, A. Revcolevschi, Phys. Rev. B 57 (1998) R5571.

[2] Y. Endoh, K. Hirota, S. Ishihara, S. Okamoto, Y. Murakami, A. Nishizawa, T. Fukuda, H. Kimura, H. Nogiri, K. Kaneko, S. Maekawa, Phys. Rev. Lett. 82 (1999) 4328.
[3] J.S. Zhou, J.B. Goodenough, A. Asamitsu, Y. Tokura, Phys. Rev. Lett. 79 (1997) 3234.
[4] M. Sasaki, H. Negeshi, M. Inoue, J. Appl. Phys. 59 (1986) 796.
[5] A. Pimenov, M. Biberacher, D. Ivannikov, A. Loidl, V.Yu. Ivanov, A.A. Mukhin, A.M. Balbashov, Phys. Rev. B 62 (2000) 5685.
[6] H.L. Ju, J. Gopalakrishnan, J.L. Peng, G.C. Xiong, Qi Li, T. Venkatesan, R.L. Greene, Phys. Rev. B 51 (1995) 6143.
[7] Y. Okimoto, T. Katsufuji, T. Ishikawa, A. Urushibara, T. Arima, Y. Tokura, Phys. Rev. Lett. 75 (1995) 109.
[8] M. G. Blamire, B.S. Teo, J.H. Durrell, N.D. Mathur, Z.H. Barber, J.L. Manus Driscoll, L.F. Cohen, J.E. Evetts, J. Magn. Magn Mater. 191 (1999) 359 (strains).
[9] L.A. Tikhonova, G.I. Samal, P.P. Zhuk, A.A. Tonoyan, A.A. Vecher, Izv. Akad. Nauk SSSR, Neorg. Mater. 26 (1990) 189.
[10] K. Steenbeck, T. Eick, K. Kirsch, H.G. Schmidt, E. Steinbeiß, Appl. Phys. Lett. 73 (1998) 2506.
[11] M. Paraskevopoulos, F. Mayr, J. Hemberger, A. Loidl, R. Heichele, D. Maurer, V. Müller, A.A. Mukhin, A.M. Balbashov, J. Phys. C 12 (2000) 3993.
[12] S. Uhlenbruck, R. Teipen, R. Klingeler, B. Büchner, O. Friedt, M. Hücker, H. Kierspel, T. Niemöller, L. Pinsard, A. Revcolevschi, R. Gross, Phys. Rev. Lett. 82 (1999) 185.
[13] J. Liebe, K. Heinemann, K. Bärner, I.V. Medvedeva, Yi Tang, S. Dong, R. Braunstein, Mat. Sci. Eng. B 47 (1997) 244.
[14] H.L. Ju, C. Kwon, Qi Li, R.L. Greene, T. Venkatesan, Appl. Phys. Lett. 65 (1994) 2108.
[15] J. Liebe, L. Haupt, A. Kattwinkel, N. Hamad, G.H. Rao, K. Bärner, E. Gommert, J. Wecker, R.v. Helmolt, R. Braunstein, G.S. Sun, I.V. Medvedeva, J. Magn. Magn. Mater. 196 (1999) 484.
[16] J. Liebe, E. Kraus, L. Haupt, P. Mandal, K. Bärner, R.v. Helmolt, Appl. Phys. Lett. 68 (1996) 2343.
[17] J. Liebe, H. Kang, L. Haupt, P. Mandal, I.V. Medvedeva, K. Bärner, A. Poddar, E. Gmelin, Physica B 239 (1997) 322.
[18] E. Kraus, K. Heinemann, K. Bärner, F.A. Khan, I.V. Medvedeva, H. Schicketanz, P. Terzieff, Phys. Stat. Sol. (A) 177 (2000) 547.
[19] M. Jaime, M.B. Salamon, K. Petitt, M. Rubinstein, R.E. Treece, J.S. Horwitz, D.B. Chrisez, Appl. Phys. Lett. 68 (1996) 1576.
[20] H. Kang, P. Mandal, I.V. Medvedeva, K. Bärner, A. Poddar, E. Gmelin, Phys. Stat. Sol. (A) 163 (1997) 465.
[21] H. Kang, K. Bärner, I.V. Medvedeva, P. Mandal, A. Poddar, E. Gmelin, J. Alloys Compounds 267 (1998) 1.
[22] L. Haupt, R.v. Helmolt, U. Sondermann, K. Bärner, Y. Tang, E.R. Giessinger, E. Ladizinsky, R. Braunstein, Phys. Lett. A 165 (1992) 473.
[23] E.A. Livesay, R.N. West, S.B. Dugdale, G. Santi, T. Jarlborg, J. Phys. C 11 (1999) L279.
[24] I.S. Efimov, V.I. Anisimov, G.A. Sawatzky, Phys. Rev. Lett. 82 (1999) 4264.
[25] J. Volger, Physica XX (1954) 49.
[26] V.E. Arkhipov, V.S. Gaviko, A.V. Korolyov, V.E. Naish, V.V. Marchenkov, Y.M. Mukovskii, S.G. Karaboshev, D.A. Shulyatev, A.A. Asenov, J. Magn. Magn. Mater. 196–97 (1999) 539.
[27] U. Neitzel, K. Bärner, J. Phys. C 11 (1978) 4975.
[28] T. Kasuya, Progr. Theor. Phys. 22 (1959) 372.
[29] Y.S. Touloukian, Thermal Conductivity, Metals and Alloys, Plenum, New York, 1970.
[30] A. Poddar, P. Muruguraj, R. Fischer, E. Gmelin, K. Bärner, L. Haupt, P. Mandal, G.H. Rao, Physica B 254 (1998) 21.
[31] E. Kraus, K. Bärner, K. Heinemann, T. Kanomata, I.V. Mevedeva, P. Mandal, E. Gmelin, Phys. Stat. Sol. (A) 157 (1996) 449.
[32] A. Urushibara, Y. Moritomo, T. Arima, A. Asamitsu, G. Kido, Y. Tokura, Phys. Rev. B 51 (1995) 14103.
[33] P. Mandal, Phys. Rev. B 61 (2000) 14675.
[34] A. Asamitsu, Y. Moritomo, Y. Tokura, Phys. Rev. B 53 (1996) R2952.
[35] M.F. Hundley, J.J. Neumeier, Phys. Rev. B 55 (1997) 11511.
[36] J.L. Cohn, J.J. Neumeier, C.P. Popoviciu, K.J. McClellan, Th. Leventouri, Phys. Rev. B 56 (1997) R8495.
[37] H. Fujishiro, M. Ikebe, Physica B 263–264 (1999) 691.
[38] D.W. Visser, A.P. Ramirez, M.A. Subramanian, Phys. Rev. Lett. 78 (1997) 3947.
[39] Baoxing Chen, A.G. Rojo, C. Uher, H.L. Ju, R.L. Greene, Phys. Rev. B 55 (1997) 15471.
[40] R.D. Barnard, Thermoelectricity of Metals and Alloys, Taylor & Francis, London, 1972, 1ff.
[41] G.H. Rao, J.R. Sun, A. Kattwinkel, L. Haupt, K. Bärner, E. Schmitt, E. Gmelin, Physica B 269 (1999) 379.
[42] A. Kattwinkel, E. Kraus, Ch. Kleeberg, T. Gron, K. Bärner, Acta Physica Polonica A 93 (1998) 745.
[43] E. Kraus, Diploma Thesis, Göttingen 1995.
[44] R.R. Heikes, Thermoelectricity, Wiley Interscience, 1961.